

# Self-Powered Ultrasensitive Nanowire Photodetector Driven by a Hybridized Microbial Fuel Cell\*\*

Qing Yang, Ying Liu, Zetang Li, Zongyin Yang, Xue Wang, and Zhong Lin Wang\*

Nanostructures are promising materials for photodetection, with advantages of high sensitivity, fast response speed, and low energy consumption.<sup>[1]</sup> However, until now, highly sensitive nanostructure-based photodetectors have been designed to be driven by external power sources, which not only largely increase the system size but also greatly limit their mobility and independence for applications in areas such as large-area wireless environmental sensing, chemical and biosensing, and in situ medical therapy monitoring. One of the goals of nanotechnology is to build a nanosystem that can function as a living species, with capabilities of sensing, controlling, communicating, and actuating/responding.<sup>[2]</sup> Such a nanosystem is composed of not only nanodevices but also a power source. For instance, implanted nanoscale biosensors for monitoring diabetes and blood pressure require a nontoxic power source without adding too much weight and size. Although a battery or energy storage unit may be a choice for powering nanodevices, harvesting energy from the environment is an essential solution for building a self-powered nanodevice/nanosystem, which is indispensable for sustainable operation of a large portion of the sensor network.<sup>[2]</sup> For example, a self-powered nanoscale photodetector network is highly desired for waste-water and air-pollution monitoring systems that feature low energy consumption, low cost, and high sensitivity.<sup>[3]</sup> Recently, a self-powered UV detector driven by a pn heterojunction photocell was demonstrated,<sup>[4]</sup> but the limitation of the detectable light intensity is very high (ca. 200 W cm<sup>-2</sup>). However, for environmental monitoring

and medical therapy treatment, weak light detection is much more desired. Herein we demonstrate an integrated system of a self-powered ultrasensitive single-nanowire-based multi-color photodetector driven by a high-efficiency microscale microbial fuel cell (MFC) that was fabricated using a carbon fiber–ZnO nanowire hybridized structure. One microscale MFC can power an ultrasensitive nanowire photodetector (NRPD) with a responsivity of more than 300 A W<sup>-1</sup> and a detection limit as low as nW/cm<sup>2</sup>. The noise-equivalent power (NEP) of the self-powered NRPD for detection of UV, blue, and green light at 10 Hz is about 5.0 × 10<sup>-18</sup>, 1.5 × 10<sup>-17</sup>, and 2.8 × 10<sup>-17</sup> W Hz<sup>-1/2</sup>, respectively, indicating extremely high sensitivity of the self-powered nanosystem, which is compatible with those of quantum dots and polymer-nanowire-based photodetectors. Thus, it opens exciting opportunities for self-powered detectors with a wide spectral range of high responsivity and high resolution. Our self-powered nanosystem may find a variety of applications in medical therapy, environmental monitoring, defense technology, and personal electronics; for example, light dosimetry measurement in photodynamic therapy and contamination detection in polluted water. Furthermore, parallel or series connection of a hybridized fuel cell can be adopted to improve the output similar to the integration of nanogenerator, as carried out previously.<sup>[5]</sup>

Our self-powered nanosystem is fabricated by integrating a single-fiber NW hybrid-structured MFC with a single CdS NRPD in series (Figure 1a; Supporting Information, Figure S1). The MFC uses a carbon fiber that is radially surrounded with densely packed ZnO NWs (Figure 1b). The principle of the MFC is shown in Figure 2a. The carbon fiber (5 μm in diameter) acts not only as the substrate onto which the ZnO NWs were grown but also as an electrode (indicated as electrode EII in Figure 1a).<sup>[6]</sup> Densely packed ZnO NWs with lengths of about 250 nm were grown around the carbon fiber by a physical vapor deposition method.<sup>[6]</sup> A thin layer of Nafion was spin-coated on the fiber-NW hybrid structure as the anion exchange membrane in the MFC. Then a millimeter-diameter solution micropool was constructed by squeezing poly(methyl methacrylate) (PMMA) polymer solution onto the Nafion film in a ring dam shape to form a micropool (the inner diameter ranges from 1 to 5 mm, the thickness is about 1 mm, and the volume is less than 20 μL). The micropool not only keeps the yeast solution near the hybrid structure, but also improves the stability of the MFC. Yeast and glucose were mixed in solution and dripped into the micropool. The MFC was connected to the outer circuit by two electrodes. The first electrode (EI) was placed on the top surface of the yeast solution, the other electrode (EII) was connected to one end of the carbon fiber where ZnO NWs

[\*] Dr. Q. Yang,<sup>[†]</sup> Y. Liu,<sup>[†]</sup> Z. Li,<sup>[†]</sup> X. Wang, Prof. Z. L. Wang  
School of Materials Science and Engineering  
Georgia Institute of Technology  
Atlanta, GA 30332-0245 (USA)  
E-mail: zlwang@gatech.edu  
Homepage: <http://www.nanoscience.gatech.edu>  
Dr. Q. Yang,<sup>[†]</sup> Z. Yang  
State Key Laboratory of Modern Optical Instrumentation  
Department of Optical Engineering, Zhejiang University  
Hangzhou 310027 (P.R. China)  
Prof. Z. L. Wang  
Beijing Institute of Nanoenergy and Nanosystems, Chinese Academy of Sciences, Beijing (P.R. China)

[†] These authors contributed equally to this work.

[\*\*] The authors thank the BES, DOE, NSF, the U.S. Air Force, and the NSFC (61177062) and the Knowledge Innovation Program of Chinese Academy of Sciences (KJCX2-YW-M13) for support. The authors would like to thank Dr. Caofeng Pan for insightful discussions, and Derek Yeung for assistance.



Supporting information for this article, including methods for NW growth, device fabrication, and measurements, is available on the WWW under <http://dx.doi.org/10.1002/anie.201202008>.

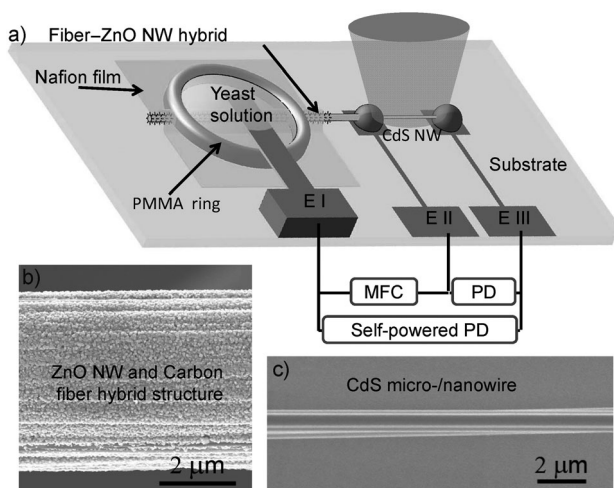


**Figure 1.** Experimental design of the self-powered photodetector system. a) Illustration of a self-powered nanosystem composed of a microbial fuel cell (MFC) and a nanowire (NW) photodetector (PD). E = electrode. b) SEM image of a carbon fiber covered with densely packed ZnO NWs, which was used for fabricating the MFC. c) SEM image of a CdS wire used for fabricating the photodetector.

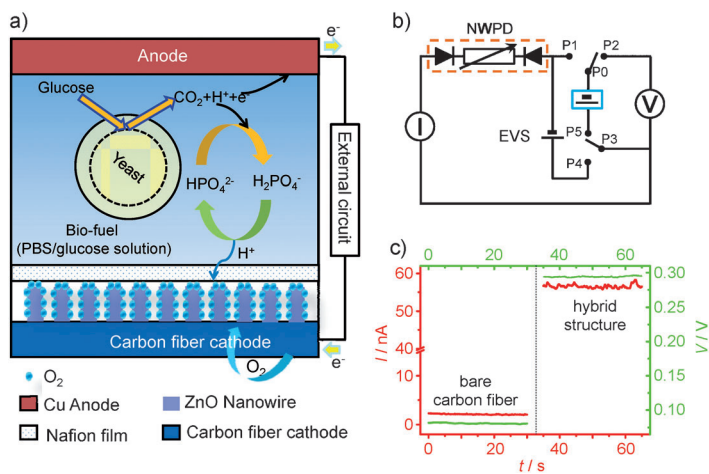


**Figure 2.** a) Principle of a MFC based on fiber-NW hybrid structure (see text for details). b) Circuit diagram used for integrating a single hybrid-structured MFC and a NWPD. EVS = external voltage source; blue = MFC. The diodes at the two ends of the device represent the local Schottky contacts between CdS and metal electrodes. c) Open-circuit voltage ( $V_{oc}$ , green) and short-circuit current ( $I_{sc}$ , red) of the hybrid-structured MFC and bare carbon fiber based MFC.

were etched away by an HCl solution. This is the power unit for the system.

The NWPD was a single CdS NW (Figure 1c), which was connected in series with the carbon fiber using silver paste at E II; the third electrode (E III) at the other end of the CdS NW was connected to the electrical measurement system. Using a circuit as shown in Figure 2b, the performance of the MFC and the photodetector was characterized separately and as a system. The entire MFC was covered by a black box made from light-absorbing materials, so that the light was shed only on the CdS NW. Monochromatic UV, blue, or green light was used to test the performance of the photodetector.

The working principle of a MFC is shown in Figure 2a. Glucose was decomposed by yeast to form CO<sub>2</sub> and electron-proton pairs. The electrons produced in the microorganism solution are transferred to the anode and subsequently through an external circuit to the cathode, whilst protons or phosphate anions migrate from anode to the cathode through the separator membrane. At the cathode, H<sup>+</sup> and electron recombine with an oxygen molecule to form H<sub>2</sub>O. A separator is an important part to ensure an efficient and sustainable operation of an MFC. The paradox of ion transfer and oxygen permeation is the major constraint for most separators in MFCs.<sup>[7]</sup> Our MFC however is based on a hybridized structure of carbon fiber-ZnO NWs, which has increased ion transfer and avoids simultaneous oxygen permeation. As shown in Figure 2a, a porous membrane rather than a smooth film will form on the ZnO NW-coated carbon fiber when spin coating Nafion film, which allows various charged or neutral species to pass through efficiently and leads to easier ion transfer.<sup>[7]</sup> On the other hand, oxygen is adsorbed and immobilized on the ZnO nanowire surfaces, as represented by blue spheres on the ZnO nanowire surfaces. Thus, the oxygen permeation through the membrane is reduced. These two advantages may allow the hybrid-structured MFC to give a higher output.

The performance of the MFC is characterized by measuring the short-circuit current  $I_{sc}$  and open-circuit voltage  $V_{oc}$ . Once a drop of yeast solution was dripped into the micropool, the MFC started to generate a DC output. A typical output of the MFC is shown in Figure 2c and Figure S3; the  $I_{sc}$  is about 56 nA, the  $V_{oc}$  is about 295 mV, and the corresponding power density is about 30 W m<sup>-2</sup> of electrode geometry area, while the performance reported for μL- and sub-μL-scale MFC is limited by low volumetric power density owing to its high internal resistance.<sup>[8]</sup> The output power density of our MFC is among the best of its kind reported to date.<sup>[8]</sup>

We found that the ZnO NWs around the carbon fiber may play an important role for the enhanced performance of our microsize MFC. For comparison purposes, a MFC was fabricated using a bare carbon fiber without ZnO NWs following the same procedures as for the hybrid structured MFC. The corresponding  $I_{sc}$  was about 2 nA, and the  $V_{oc}$  was about 80 mV, and the corresponding power density was 0.29 W m<sup>-2</sup> of the electrode geometry area (Figure 2c), which are two orders of magnitude lower than that of the hybrid structured MFC. Thus, the significant enhancement in performance of our hybrid structured MFC may originate from the increased surface area and the absorption of oxygen at ZnO NW surfaces.

By integrating a MFC with a CdS NWPD,<sup>[1g,9]</sup> a self-powered photodetector can be achieved. The output voltage of the MFC was about 295 mV, which was high enough to drive a NWPD (Figure 3; Supporting Information, Figure S4). The self-powered nanosystem shows an excellent response to solar light, with a response time of about 30 ms and decaying time of about 40 ms (Supporting Information, Figure S4a,b). The photocurrent arises from the photoconductivity of the CdS NW and the shrinkage of the depletion region of the Schottky contact.<sup>[1f,g,9,10]</sup> The fast response time

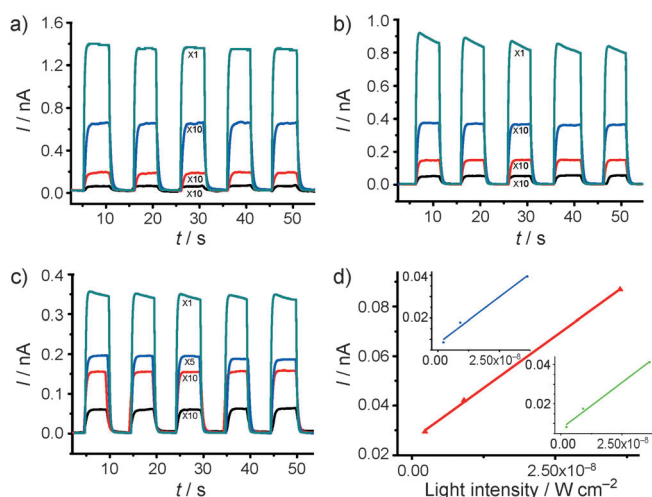


**Figure 3.** UV-blue-green multicolor detection by a single CdS NWPD driven by a single hybrid-structured MFC. a) UV light (372 nm); b) blue light (486 nm); c) green light (548 nm). Light intensities (light power illuminated onto the CdS wire): black  $2.3 \times 10^{-9}$  (25 fW), red  $9.1 \times 10^{-9}$  (100 fW), blue  $3.6 \times 10^{-8}$  (400 fW), and green  $1.6 \times 10^{-4}$  W cm $^{-2}$  (1.7 nW). d) Photocurrent as a function of the excitation intensity on the CdS NW that was illuminated by UV, blue, and green light (curves correspond to the color of the light).

results from the Schottky contact<sup>[1f]</sup> and high crystallinity of the CdS NW.<sup>[11]</sup> A Schottky contacted device has been proven to have a much higher sensitivity and much faster responsivity than an ohmic contacted device for a gas, chemical, and biosensor.<sup>[10]</sup> Regarding the intensity dependence of measured current and derived responsivity for solar detection (Supporting Information, Figure S4c,d), the responsivity decreases at high light intensity owing to the elimination of the Schottky barrier and hole-trapping saturation at strong light intensities.<sup>[1e,g]</sup>

Apart from solar light detection, our self-powered photodetector can be used to detect multicolor light ranging from red light to UV light. For the integration system of the hybrid structured MFC and the CdS NW connected in series (Figure 1a), if light irradiation on the CdS NW is turned off, the system current had a leakage current less than 1 fA. Once the UV light with an intensity of about  $1.6 \times 10^{-4}$  W cm $^{-2}$  shed on the CdS NW, the system current increased immediately to 1.4 nA (Figure 3a). The on-off cycles have remarkable reproducibility.

Our self-powered nanosystem can detect light down to a nW/cm $^2$  level (fW light illuminating onto the NW). The responsivity for UV, blue, and green light with intensity of  $2.3$  nW cm $^{-2}$  (equal to 25 fW light illumination onto the NW) of the system were 1180, 344, and 332 AW $^{-1}$ , respectively, which is two to three orders of magnitude higher than that received using a nitride based metal-semiconductor-metal photodetector<sup>[12]</sup> and a silicon NW photodetector.<sup>[13]</sup> Figure 3d shows the photocurrent versus light intensity for UV, blue, and green light, respectively, indicating that the photocurrent increased linearly with the optical power for sub- $\mu$ W/cm $^2$  light detection. The spectral photoresponse of the self-powered nanosystem (Supporting Information, Figure S5b)

showed that the responsivity depended on light wavelength. The responsivity for UV, blue, and green light was much higher than that for red light, as the photon energy of red light is less than the band gap of CdS, and thus the generation of electron-hole pairs was less efficient.

The figure of merit of a photodetector is the NEP, that is, the minimum radiant power that a detector can distinguish from noise. It is difficult to measure the signal when the signal-to-noise ratio is unity. Therefore, it is customary to make the measurement at a high level of incident radiation and calculate the NEP from the following equation:<sup>[1c,14]</sup>

$$\text{NEP} = \frac{I_N}{R\sqrt{\Delta f}} \quad (1)$$

where  $I_N$  is root-mean-square value of the noise current at output of the photodetector,  $R$  is responsivity of the photodetector, and  $\Delta f$  is the electrical bandwidth in Hz. Frequency-dependent responsivity and the noise-equivalent power of the self-powered nanosystem are shown in Figure 4a and 4b, respectively. Surprisingly, we found that the noise current of the NWPD driven by a hybridized MFC is about one order of magnitude lower than that driven by an external voltage provided by a function generator, especially at frequencies that are overtones or combination bands of 60 Hz (Figure 4b, inset image), which is due to the small size, good stability of the microscale MFC, and isolated properties of the nano-

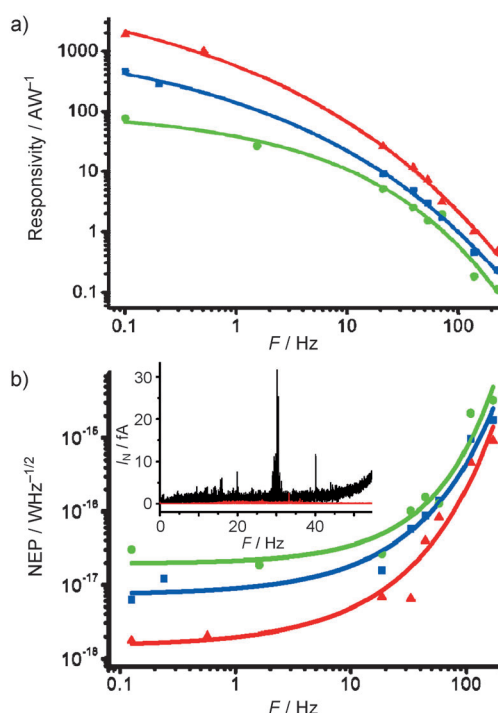


**Figure 4.** Frequency-dependent performance of the self-powered multi-color NWPD. a) Responsivity versus modulation frequency  $F$  under  $2.3 \times 10^{-9}$  W cm $^{-2}$  UV, blue, and green light illumination. Lines: data fitting. b) Noise-equivalent power (NEP) versus modulation frequency  $F$  of the self-powered NWPD for different color light detection. Inset: noise current  $I_N$  of the NWPD driven by a hybridized MFC (red) and by a 0.3 V external voltage source (black) provided through a function generator at a bandwidth of 90 Hz (from 10 to 100 Hz).

system. The NEP of the self-powered NRPD for detection of UV, blue, and green light at 10 Hz is about  $5.0 \times 10^{-18}$ ,  $1.5 \times 10^{-17}$ , and  $2.8 \times 10^{-17}$   $\text{W Hz}^{-1/2}$ , respectively, which is two to three orders lower than previous reports,<sup>[1b,c,14,15]</sup> and means that our self-powered NRPD has the potential to detect light down to a sub-fW level. The thermal noise of the device is estimated by the form  $(4kT\Delta f/R_e)^{1/2}$  to be  $2.5 \times 10^{-18}$   $\text{A Hz}^{-1/2}$ , where  $k$  is the Boltzman constant,  $T$  is the temperature,  $R_e$  is the resistance of the detector in the dark, and  $\Delta f$  is the percentage bandwidth. While the shot noise limit  $(2qI_N\Delta f)^{1/2}$  is estimated to be  $5.9 \times 10^{-18}$   $\text{A Hz}^{-1/2}$ , where  $q$  is the electron charge and  $I_N$  is the dark noise current. Our self-powered NRPD approaches the shot noise limit at 10 Hz.<sup>[1c]</sup>

In summary, we have demonstrated a self-powered, ultrasensitive multicolor photodetector driven by a hybrid-structured microbial fuel cell. A single-fiber MFC generates a DC output about  $V_{oc} = 295$  mV and  $I_{sc} = 56$  nA, and provides a power density of  $30 \text{ W m}^{-2}$  of electrode geometry area. The self-powered photodetector can detect down to about nW/ $\text{cm}^2$  light intensity with a responsivity more than  $300 \text{ A W}^{-1}$ , which is two to three orders of magnitude higher than that achieved using a conventional metal–semiconductor–metal photodetector. The NEP of the self-powered NRPD for detection of UV, blue, and green light at 10 Hz is about  $5.0 \times 10^{-18}$ ,  $1.5 \times 10^{-17}$ , and  $2.8 \times 10^{-17}$   $\text{W Hz}^{-1/2}$ , respectively. The self-powered high-sensitive nanosystem has potential applications for wireless day- and nighttime environmental surveillance, biological sensing, medical treatment, and defense technology.<sup>[3,8e,16]</sup> For example, in environmental monitoring, a high-sensitive nanowire photodetector driven by bacteria has high potential to detect fluorescence of the contamination in recycled water system, where rapid and highly sensitive detector is urgently required.<sup>[3]</sup>

Received: March 13, 2012

Revised: April 30, 2012

Published online: May 29, 2012

**Keywords:** fuel cells · microbes · nanotechnology · noise equivalent power · photodetectors

- [1] a) M. W. Knight, H. Sobhani, P. Nordlander, N. J. Halas, *Science* **2011**, 332, 702–704; b) S. Keuleyan, E. Lhuillier, V. Brajuskovic, P. Guyot-Sionnest, *Nat. Photonics* **2011**, 5, 489–493; c) G. Konstantatos, J. Clifford, L. Levina, E. H. Sargent, *Nat. Photonics* **2007**, 1, 531–534; d) P. Irvin, Y. Ma, D. F. Bogorin, C. Cen, C. W. Bark, C. M. Folkman, C. B. Eom, J. Levy, *Nat. Photonics*

- 2010**, 4, 849–852; e) C. Soci, A. Zhang, B. Xiang, S. A. Dayeh, D. P. R. Aplin, J. Park, X. Y. Bao, Y. H. Lo, D. Wang, *Nano Lett.* **2007**, 7, 1003–1009; f) J. Zhou, Y. D. Gu, Y. F. Hu, W. J. Mai, P. H. Yeh, G. Bao, A. K. Sood, D. L. Polla, Z. L. Wang, *Appl. Phys. Lett.* **2009**, 94, 191103; g) Q. Yang, X. Guo, W. H. Wang, Y. Zhang, S. Xu, D. H. Lien, Z. L. Wang, *ACS Nano* **2010**, 4, 6285–6291; h) H. Kind, H. Yan, B. Messer, M. Law, P. Yang, *Adv. Mater.* **2002**, 14, 158–160; i) W. Wei, X. Bao, C. Soci, Y. Ding, Z. L. Wang, D. Wang, *Nano Lett.* **2009**, 9, 2926–2934.
- [2] a) Z. L. Wang, *Sci. Am.* **2008**, 298, 82–87; b) C. Pan, Y. Fang, H. Wu, M. Ahmad, Z. Luo, Q. Li, J. Xie, X. Yan, L. Wu, Z. L. Wang, J. Zhu, *Adv. Mater.* **2010**, 22, 5388–5392; c) Y. Hu, Y. Zhang, C. Xu, G. Zhu, Z. L. Wang, *Nano Lett.* **2010**, 10, 5025–5031; d) B. Tian, X. Zheng, T. J. Kempa, Y. Fang, N. Yu, G. Yu, J. Huang, C. M. Lieber, *Nature* **2007**, 449, 885–890.
- [3] a) R. K. Henderson, A. Baker, K. R. Murphy, A. Hambly, R. M. Stuetz, S. J. Khan, *Water Res.* **2009**, 43, 863–881; b) M. A. Shannon, P. W. Bohn, M. Elimelech, J. G. Georgiadis, B. J. Marinas, A. M. Mayes, *Nature* **2008**, 452, 301–310.
- [4] Y. Bie, Z. Liao, H. Zhang, G. Li, Y. Ye, Y. Zhou, J. Xu, Z. Qin, L. Dai, D. Yu, *Adv. Mater.* **2011**, 23, 649–653.
- [5] a) S. Xu, Y. Qin, C. Xu, Y. Wei, R. Yang, Z. L. Wang, *Nat. Nanotechnol.* **2010**, 5, 366–373; b) G. Zhu, R. Yang, S. Wang, Z. L. Wang, *Nano Lett.* **2010**, 10, 3151–3155.
- [6] Z. Li, Z. L. Wang, *Adv. Mater.* **2011**, 23, 84–89.
- [7] W. Li, G. Sheng, X. Liu, H. R. Yu, *Bioresour. Technol.* **2011**, 102, 244–252.
- [8] a) H. Y. Wang, A. Bernard, C. Y. Huang, D. J. Lee, J. S. Chang, *Bioresour. Technol.* **2011**, 102, 235–243; b) S. R. Crittenden, C. J. Sund, J. J. Sumner, *Langmuir* **2006**, 22, 9473–9476; c) F. Qian, M. Baum, Q. Gu, D. E. Morse, *Lab Chip* **2009**, 9, 3076–3081; d) E. Kjeang, N. Djalili, D. Sinton, *J. Power Sources* **2009**, 186, 353–369; e) O. Schaetzle, F. Barriere, K. Baronian, *Energy Environ. Sci.* **2008**, 1, 607–620.
- [9] Y. Liu, Q. Yang, Y. Zhang, Z. Yang, Z. L. Wang, *Adv. Mater.* **2012**, 14, 1410–1417.
- [10] a) T. Wei, P. Yeh, S. Lu, Z. L. Wang, *J. Am. Chem. Soc.* **2009**, 131, 17690–17690; b) P. Yeh, Z. Li, Z. L. Wang, *Adv. Mater.* **2009**, 21, 4975–4978.
- [11] F. Gu, Z. Yang, H. Yu, J. Xu, P. Wang, L. Tong, A. Pan, *J. Am. Chem. Soc.* **2011**, 133, 2037–2039.
- [12] C. Chen, K. Wang, S. Tsai, H. Chien, S. Wu, *Jpn. J. Appl. Phys.* **2010**, 49, 04DG06.
- [13] M. M. Adachi, K. Wang, F. Chen, K. S. Karim, *Proc. SPIE-Int. Soc. Opt. Eng.* **2010**, 7622, 76224M.
- [14] X. Gong, M. Tong, Y. Xia, W. Cai, J. S. Moon, Y. Cao, G. Yu, C. Shieh, B. Nilsson, A. J. Heeger, *Science* **2009**, 325, 1665–1667.
- [15] H. Luquet, L. Gousskov, M. Perotin, A. Jean, D. Magallon, *J. Appl. Phys.* **1988**, 64, 6541–6545.
- [16] a) Y. Wei, J. Song, Q. Chen, *Photochem. Photobiol. Sci.* **2011**, 10, 1066–1071; b) J. Chen, L. Keltner, J. Christophersen, F. Zheng, M. Krouse, A. Singhal, S. S. Wang, *Cancer J.* **2002**, 8, 154–163.